

FRACTURE OF CONCRETE COVER - ITS EFFECT ON TENSION STIFFENING AND MODELING -

(Reprinted from proceedings of JSCE, No.613/V-42, February 1999)



Hamed SALEM



Bernhard HAUKE



Koichi MAEKAWA

The aim of this study is to investigate the effect of insufficient concrete cover on the tension stiffness of reinforced concrete. Splitting cracks are predicted by simultaneously solving for equilibrium among radial bond stresses, softening tensile stresses of splitting concrete planes, and transverse stress on the reinforcement. The behavior of bond after splitting cracks occur is the point of the study. An analytical model is derived from the micro-bond characteristics. An experimental program was carried out to verify the proposed post-crack bond model, and the analysis is in fairly good agreement with reality

Keywords: Bond-slip-strain, tension stiffening, crack spacing, confining pressure, splitting crack, cover

Hamed M. M. Salem is an assistant professor at the Structural Engineering Department, Cairo University, Giza, Egypt. He obtained his Ph.D. from the University of Tokyo in 1998. After obtaining his Ph.D., he worked as a JSPS post-doctoral fellow in the Concrete Laboratory, The University of Tokyo. His research interests relate to nonlinear mechanics and the constitutive laws of reinforced concrete as well as the seismic analysis of reinforced concrete. He is a member of the JSCE.

Bernhard HAUKE is an engineer at HOCHTIEF AG in Frankfurt, Germany. He obtained his Ph.D. from the University of Tokyo in 1998. His research interests relate to the nonlinear mechanics of reinforced concrete and analysis of steel composite structures. He is a member of the JSCE.

Koichi Maekawa is a professor at The University of Tokyo. He obtained his D.Eng. from the University of Tokyo in 1985. His research interests relate to nonlinear mechanics and the constitutive laws of reinforced concrete as well as seismic analysis of structures and concrete thermodynamics. He is a member of the JSCE.

1. INTRODUCTION

When there is insufficient concrete, longitudinal “splitting” cracks, form parallel to the reinforcing bars. The occurrence of these cracks is a result of three-dimensional bond transfer mechanisms. The lugs of deformed bars induce bearing stresses in the surrounding concrete, resulting in conical compressive struts as shown in **Fig. 1**. The conical bond actions between bar and concrete can be resolved into radial and tangential components. Usually, the tangential component per unit area of the reinforcing bar's surface is called the bond stress, whereas the radial one is called the confining stress. The radial stresses may be seen as analogous to hydraulic pressure acting on a thick-walled concrete ring. When the tensile ring stress illustrated in **Fig. 1** exceeds the cracking strength, a splitting crack is formed as shown in **Fig. 2**.

The bond behavior of concrete with such cracks was studied by Gambarova et al.⁵⁾. Gambarova tested specimens with artificially induced splitting cracks. By relating the splitting crack width to the confining pressure on the bars, an empirical formula was proposed for bond stresses after longitudinal splitting of the concrete cover. Abrishami and Mitchell¹⁰⁾ studied the effect of splitting cracks on the tension stiffening of concrete. Specimens with shallow depth were targeted. Here, the concrete cover was insufficient on both sides of the reinforcing bars concerned. Most members of civil structures are deep in general and the small cover of either side of the structural reinforcement does matter. Therefore, splitting cracks would have less effect. Salem and Maekawa¹¹⁾,¹²⁾ derived macroscopic tension stiffening from local bond stress development by assuming thick cover, which would lead to the full performance of bond stress formulated by Shima et al⁹⁾.

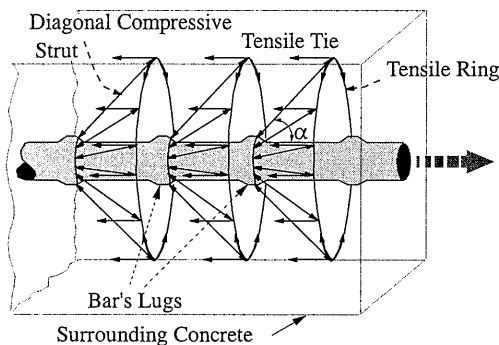


Fig. 1 Tensile ring force caused by diagonal bond struts

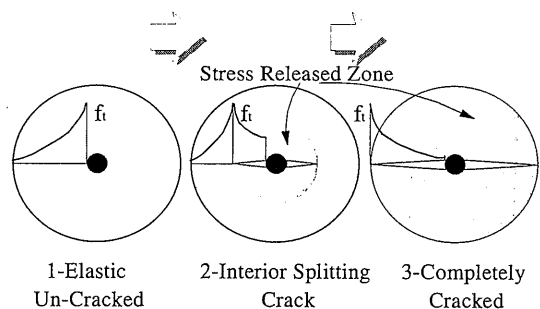


Fig. 2 Radial tensile stresses and splitting cracks

The aim of this study is to derive a smeared model for reinforced concrete in tension from microscopic behavior, taking into account the possible reduction in bond stresses due to insufficient cover accompanying longitudinal splitting cracks. This study is an extension of the authors' formulation of macro tension-stiffness^{11), 12)} covering the case where pre-matured splitting cracks are induced.

2. SPLITTING BOND STRESS

(1) Members without transverse reinforcement

The principal direction of the bond force transferred between deformed reinforcing bars and the surrounding concrete is at an angle with the bar axis. The bond forces can be resolved into radial and tangential components. Usually, the tangential component is called the bond stress, whereas the radial one is called the confining stress or pressure. The angle of inclination denoted by α (see **Fig. 1**) ranges from 45 to 80 degrees as reported by Goto²⁾. The radial stresses due to bond action act like hydraulic pressure acting on a thick-walled concrete ring.

An elastic solution for the stresses in a thick-walled cylinder subjected to internal pressure is given by Timoshenko¹⁾ and also by Avalue et al.⁹⁾ as,

$$\sigma_r = p R_{cr}^2 \left(\frac{1 - \frac{R_{max}^2}{r^2}}{R_{max}^2 - R_{cr}^2} \right) \quad \sigma_t = p R_{cr}^2 \left(\frac{1 + \frac{R_{max}^2}{r^2}}{R_{max}^2 - R_{cr}^2} \right) \quad (1)$$

where, σ_r , σ_t : radial and tangential stresses at radial distance r from the centre of the bar; p : radial pressure; R_{cr} : radius of cracked concrete zone; R_{max} : cover of concrete + $\Phi/2$; and Φ : bar diameter.

These equations are valid for uncracked concrete. However, in cracked concrete, a tension fracturing zone develops as illustrated in Fig. 3.

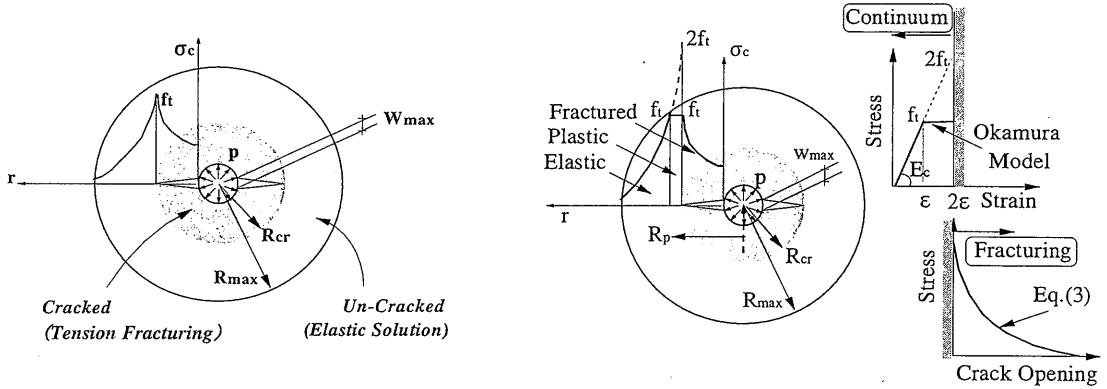


Fig. 3 Tangential stress developing in cracked and uncracked concrete

Fig. 4 Elasto-plastic and fracturing concrete in tension

According to Avalue et al.⁹⁾, the bond pressure which causes a splitting crack of radius R_{cr} can be computed by equilibrating the bond pressure p with the hoop tensile stresses in both the cracked and uncracked concrete as,

$$p = \frac{2f_t}{\Phi} \left(R_{cr} \left(\frac{R_{max}^2 - R_{cr}^2}{R_{max}^2 + R_{cr}^2} \right) + \int_{\Phi/2}^{R_{cr}} \left(\frac{\sigma_c(w(r))}{f_t} \right) dr \right) \quad (2)$$

where, f_t is the tensile strength, $w(r)$ is the splitting crack width at radius r , and $\sigma_c(w(r))$ is the residual tensile stress corresponding to a crack width equal to $w(r)$. The tension softening model adopted here is given by Uchida et al.⁷⁾ as,

$$\sigma_c(w(r)) = f_t \left(1 + 0.5 \left(\frac{f_t}{G_f} \right) w(r) \right)^{-3} \quad (3)$$

where G_f is the fracture energy ranging from 0.1 to 0.15 N/mm for plain normal concrete⁷⁾.

In Eq. 2, Avalue assumed two propagating splitting cracks. This assumption agrees with the experimental observations of Morita and Kaku³⁾ who reported that two or three splitting cracks propagate to the surface of a

concrete cylinder in pull-out tests. Moreover, in structural members, this is usually the case where splitting cracks propagate towards the side with less cover. Avalle also assumed tangential strain compatibility by equating the circumferential elongation at the surface of the reinforcing bar and at the crack propagation front with the concrete elasticity denoted by E_c as,

$$2\pi R_{cr} \frac{f_t}{E_c} = 2w_{max} + \left(2\pi \frac{\Phi}{2} - 2w_{max} \right) \frac{\sigma_c(w_{max})}{E_c} \quad (4)$$

Using **Eq. 4**, the splitting crack width at the reinforcing bar's surface, denoted by w_{max} , is computed.

A crack width distribution has to be assumed in order to integrate the second part in the right hand term of **Eq. 2**. The authors assume the splitting crack width distribution to be linear, ranging from w_{max} at the surface of the reinforcement to zero at the crack front, as follows.

$$w(r) = w_{max} \left(1 - \frac{r - \frac{\Phi}{2}}{R_{cr} - \frac{\Phi}{2}} \right) \quad (5)$$

When the splitting cracks reach the concrete surface, R_{cr} becomes equal to R_{max} . Thus, from **Eq. 2** we have the ultimate pressure, p_{ult} , as,

$$p_{ult} = \frac{2}{\Phi} \int_{\frac{\Phi}{2}}^{R_{max}} \sigma_c(w(r)) dr \quad (6)$$

By substituting **Eq. 5** into **Eq. 3** we have,

$$\sigma_c(w(r)) = f_t \left(1 + \frac{0.5f_t w_{max} [R_{max} - r]}{G_f \left[R_{max} - \frac{\Phi}{2} \right]} \right)^{-3} \quad (7)$$

Substitution of **Eq. 7** into **Eq. 6** yields,

$$p_{ult} = \frac{2f_t}{\Phi} \int_{\frac{\Phi}{2}}^{R_{max}} \left(1 + \frac{0.5f_t w_{max} [R_{max} - r]}{G_f \left[R_{max} - \frac{\Phi}{2} \right]} \right)^{-3} dr \quad (8)$$

Finally we have,

$$p_{ult} = \left(\frac{a}{2b} \right) \left(1 - \frac{1}{\left(1 + bR_{max} - \frac{b\Phi}{2} \right)^2} \right) \quad (9)$$

where,

$$a = \frac{2 f_t}{\Phi} \quad , \quad b = \frac{0.5 f_t w_{\max}}{G_f \left(R_{\max} - \frac{\Phi}{2} \right)} \quad (10)$$

The foregoing equations assume that concrete is an elastic-damaging material in tension. But in reality, the rapid relaxation of tensile stress at higher levels is observed in concrete as a time dependency, and a plastic-flow deformation may take place close to the cracking stress (Bujadham et al.¹⁴). Therefore, a simple form of concrete plasticity is introduced with respect to a yielding plateau equal to double the cracking strain, as proposed by Okamura and Maekawa⁶. **Figure 4** illustrates the idealized concrete plasticity in computing confining pressure.

The solution is derived by considering an exact elastic solution and determining the position with a tangential stress equal to f_t relative to the position with tangential stress equal to $2 f_t$. At location $r = R_{cr}$, the fictitious tangential stress equals to $2f_t$ and, for $r = R_p$, the substantial tangential stress must be the same as f_t . Then, by substituting these boundary conditions into **Eq. 1**, we have,

$$2 = \left(1 + \frac{R_{\max}^2}{R_{cr}^2} \right) \Bigg/ \left(1 + \frac{R_{\max}^2}{R_p^2} \right) \quad (11)$$

$$R_p = R_{cr} R_{\max} \sqrt{\frac{2}{R_{\max}^2 - R_{cr}^2}} \quad (12)$$

Consequently, the radial pressure p is computed as,

$$p = \frac{2 f_t}{\Phi} \left((R_p - R_{cr}) + R_p \left(\frac{R_{\max}^2 - R_p^2}{R_{\max}^2 + R_p^2} \right) + \int_{\Phi/2}^{R_{cr}} \left(\frac{\sigma_c(w(r))}{f_t} \right) dr \right) \quad (13)$$

The splitting pressure when concrete plasticity is considered is the same as that when plasticity is neglected. This is due to the fact that the contribution made by the uncracked concrete is zero when the crack finally reaches the outer surface of the concrete, as shown in **Fig. 5**.

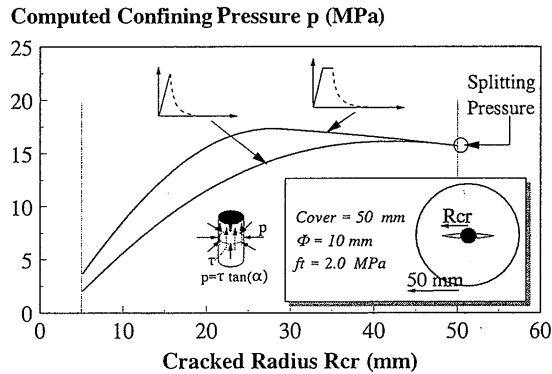


Fig. 5 Effect of concrete plasticity prior to cracking on splitting crack radius

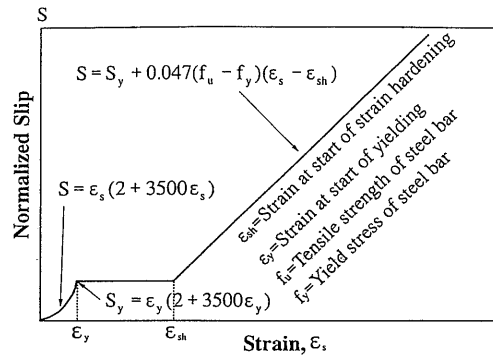
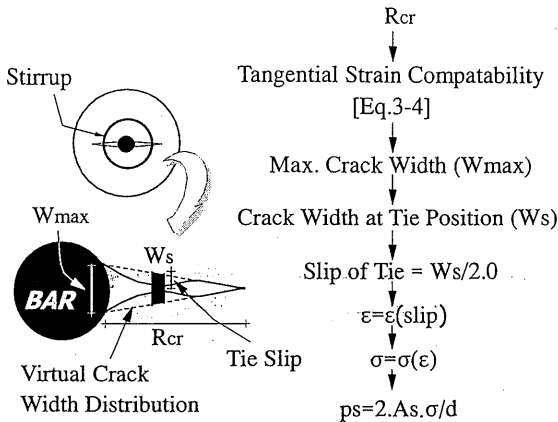


Fig. 6 Scheme for computing confining pressure due to hoop reinforcement

Fig. 7 Slip-strain relationship (Okamura and Maekawa⁶⁾)

(2) Members with transverse reinforcement

If transverse reinforcement is present, the resistance to splitting cracks increases and the confining pressure on bars is accompanied. To consider the effect of hoops, the same analysis as adopted in the previous section is used, and the confining stress produced by the hoops is added (Fig. 6). The splitting crack distribution in this case will not be linear due to the existence of hoop reinforcement, as shown in Fig. 6. The crack width vanishes at the hoop location⁸⁾. However, the real slip of the hoop reinforcement, which equals to the deformation of the concrete adjacent to the hoop, can be obtained directly from the linear distribution. Geometrically, the virtual splitting crack width at the hoop position, as computed from the linear distribution, is equal to twice the pull-out of hoops from the concrete. To compute the hoop strain at the crack location, the slip-strain relation, obtained by integrating the steel strain based on the local bond-slip-strain model, was used (Fig. 7).

Hence, the confinement provided by the hoops can be coupled with concrete fracturing. As can be seen from Fig. 8, before the tip of a splitting crack reaches the concrete surface, the confining pressure rises wherever the hoop becomes closer to the bar. This is because, the closer the hoop to the bar, the higher the load required to develop the same crack width. The authors believe that, after the crack reaches the concrete surface, a different crack width distribution may exist with a wider crack opening at the concrete surface. Hence, the closer the hoop to the bar, the lower the confining stress.

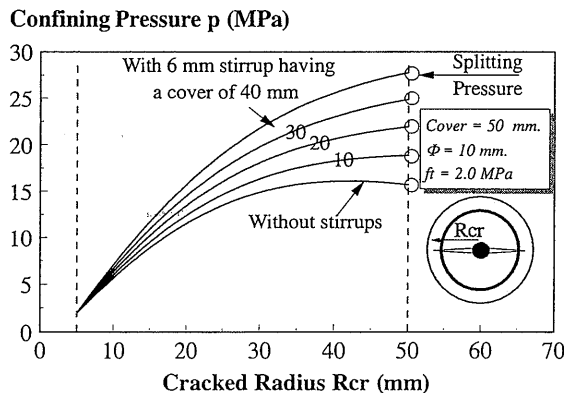


Fig. 8 Effect of hoop confinement on splitting crack radius

3. SIZE EFFECT SIMULATION

Many experimental works have exhibited a size effect in which the nominal splitting stress decreases with the increase in the bar diameter¹⁵⁾. The present model successfully simulates this size effect of splitting pressure. Since the splitting crack width is proportional to the bar diameter, as shown in Fig. 9, tension softening and hence the splitting pressure is reduced in large-scale specimens. Figure 10 shows the computed size effect on splitting for geometrically similar specimens.

4. BOND BEHAVIOR AFTER SPLITTING CRACK OCCURENCE

After splitting cracks occur, the bond stress tends to be sensitively influenced by the reinforcement confinement. This confining action may be provided by the residual stresses transmitted between the faces of the split concrete and by hoop transverse reinforcement distributed along the main bar, as illustrated in Fig. 11.

If the confining agent is not adequately apportioned around the bars, splitting cracks develop abruptly along the re-bars and a sudden splitting failure may occur. On the other hand, if adequate confining action is passively induced by the fracture of the concrete cover, the bond stress may increase until pull-out failure or rupture of re-bar as illustrated in Fig. 12. However, pull-out failure is not possible in practice. This kind of failure is possible only when the bonded length is very short, as in some experimental simulations of bond mechanisms in which only one or a few lugs are bonded.

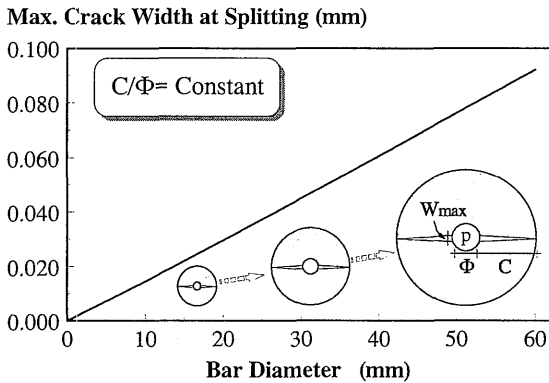


Fig. 9 Size effect on splitting crack width

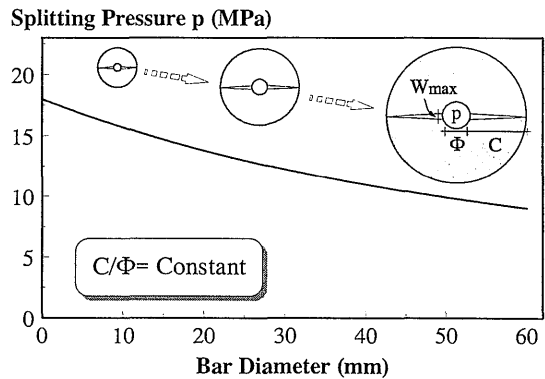


Fig. 10 Size effect on splitting pressure

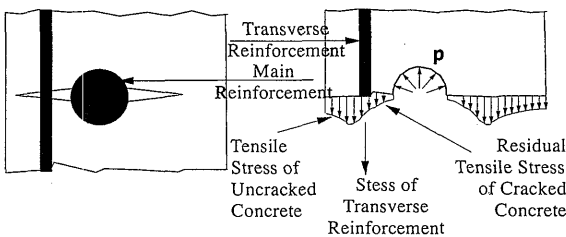


Fig. 11 Confining pressure acting on reinforcement

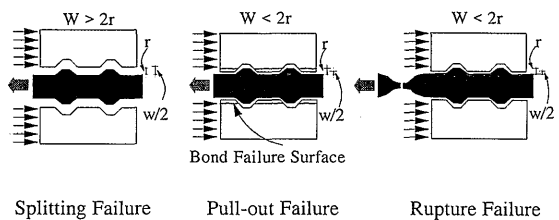


Fig. 12 Possible kinds of failure of reinforcing bars in tension

Gambarova et al.⁹⁾ developed an empirical formula for bond stress after formation of splitting cracks. Their model represents the bond stress as a function of splitting crack width, w_{max} , and bar confinement denoted by p as,

$$\tau = f'_c (0.042 - 0.288(w_{max}/\Phi)) + \left(\frac{0.258}{((w_{max}/\Phi) + 0.11)} - 1.018 \right) p \quad (14)$$

where f'_c is the compressive strength of concrete.

The bond-slip-strain model of Shima et al.⁴⁾, which is used in the analysis, does not take into account the effect of splitting cracks. In fact, in the experiments on which the model is based, splitting failure was avoided by adopting a thick concrete cover. Thus, the model of Shima is simply modified in this study by changing the intrinsic slip function as follows.

$$\tau(\epsilon, s) = \tau_0(s) \left(\frac{1}{1 + 10^5 \epsilon} \right) \quad (15)$$

$$\begin{aligned} \tau_0(s) &= f'_c k [\ln(1 + 5S)]^c && \text{before splitting} && \text{(original form)} \\ \tau_0(s) &= \tau_1 && \text{after splitting} && \text{(proposed model)} \end{aligned} \quad (16)$$

where, S is the non-dimensional slip = $1000 s/\Phi$, s is slip, Φ is bar diameter, k is constant = 0.73, c is constant = 3, and $\tau_1 = \tau_0(S=S_1)$ where S_1 is the non-dimensional slip at splitting.

The slip function after splitting might be higher or lower than the assumed one depending on the splitting crack width. The authors decided to tentatively assume plastic behavior of the slip function after splitting. This simplified model is then discussed by comparing the analytical and experimental macroscopic behavior of reinforced concrete later.

When the bond stress computed using Gambarova's model exceeds that of the original Shima model, in the case of a very small crack width, the original Shima model is used. This is because the bond stresses after splitting will not be higher than the bond stresses before splitting.

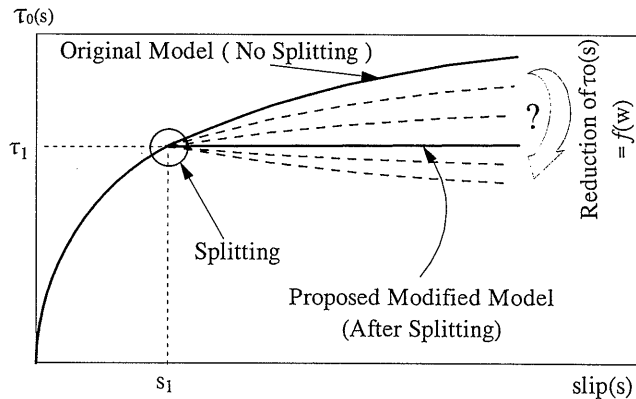


Fig. 13 Extension of Shima model⁴⁾

5. ANALYSIS ALONG AXIS OF REINFORCEMENT

Based on the microscopic bond behavior, Salem and Maekawa^{11),12)} computationally derived the macroscopic behavior of reinforced concrete in tension as illustrated in **Fig. 14**. In this analysis, local stresses of both concrete and reinforcement are evaluated. Hence, the average strains and stresses are computed over the whole of the analysis domain.

When there is insufficient concrete cover, the cover may split and a possible reduction in bond stresses also has to be checked. Here, both the Gambarova model and the modified Shima model are used with coupling as explained in the previous section. As illustrated in **Fig. 14**, five governing equations are simultaneously solved after the formation of splitting cracks. One more unknown (splitting crack width, w) accompanies the additional equation (**Eq. 14**).

Figure 15 illustrates a sample of computations, in which the splitting crack width and the bond stress are plotted along a bar of 13 mm diameter, 750 mm length, and with a concrete cover of 5 mm on both sides. The hoop tension crack width increases close to the transverse cracks, where the bond stresses are significantly decreased.

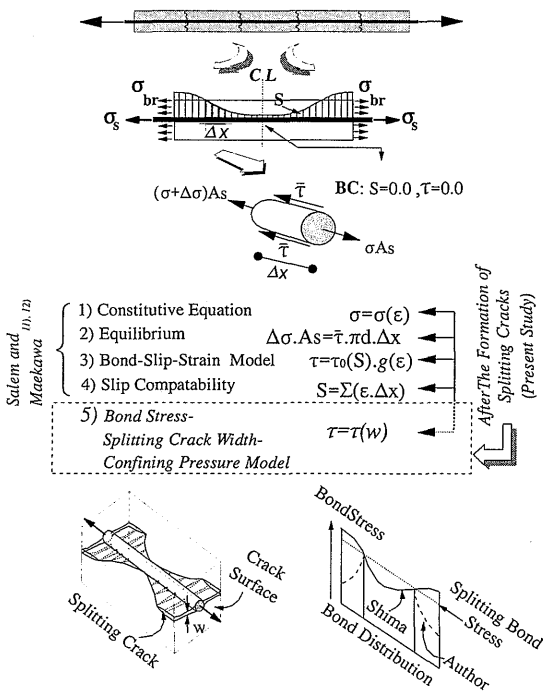


Fig.14 Scheme for solving bond governing equations with finite discretization

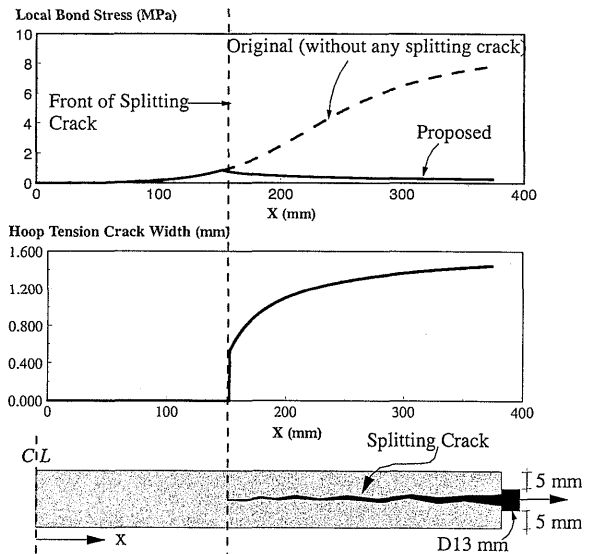


Fig.15 Analytical example for splitting crack width and reduction of bond stresses

Figure 16 illustrates the analysis of three members with the same reinforcement ratio but with different geometry and cover thickness. Cross-sections of 100×100 mm, 40×250 mm, and 30×330 mm are used. The corresponding concrete covers are 40, 10, and 5 mm, respectively. No hoop reinforcement is assumed in the analysis. For the specimens with 40 mm cover, the model predicts no splitting crack and three transverse cracks over the total length of 1,000 mm. For the 10 mm case, analysis predicts splitting cracks with only one transverse crack, while for the 5 mm case, no transverse crack is expected and longitudinal cracks are predicted. Tension stiffening is affected by the longitudinal cracks and the corresponding reduction of bond stresses. The smaller the cover concrete, the larger the reduction in tension stiffening of the concrete, as shown in **Fig. 17**.

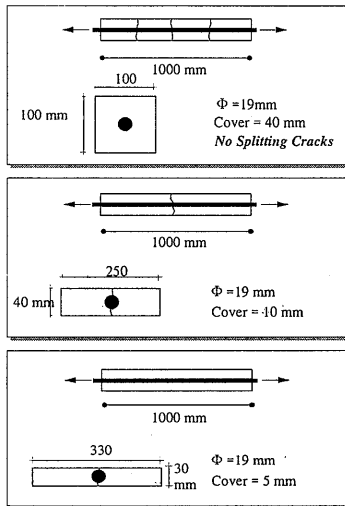


Fig.16 Case study for cover effect on tension stiffness

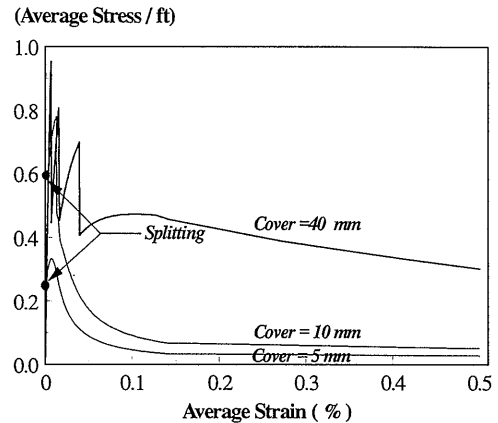


Fig.17 Case study for cover effect on tension stiffness: analytical results

6. EXPERIMENTAL VERIFICATION

(1) Abrishami and Mitchell's Experiments¹⁰⁾

For experimental verification, specimens tested by Abrishami and Mitchell¹⁰⁾ were analyzed. Abrishami tested five tension specimens. All had a length of 1,500 mm. A single reinforcing bar, with a minimum concrete cover on two faces of each specimen of 40 mm, was provided. A reinforcement ratio of 1.23 percent was used in all specimens. Reinforcing bars of diameters 11.3, 16, 19.5, 25.2, and 29.9 mm were used, respectively. **Figures 18** through **22** compare the authors' analysis with the experiments. These figures show both member behavior and the tension stiffening behavior of the concrete. It should be mentioned that the experimental tension stiffening could be computed only before yielding of reinforcing bars, since the steel is in the elastic range and the concrete contribution to load carrying can be computed by subtracting the reinforcement contribution as follows.

$$\bar{\sigma}_c = \bar{\sigma}_t - \rho(\bar{\epsilon} E_s) \quad (17)$$

$$\bar{\sigma}_t = T/A_g \quad \& \quad \bar{\epsilon} = \Delta l/l$$

where, T is the tensile load, A_g is the cross sectional area, Δl is the elongation, and l is the total length of the specimen. It has also to be mentioned that initial drying shrinkage of the specimens is not considered in the author's analysis. The analytical results show fair agreement with the experimental results.

(2) Authors' Experiments

For a further experimental verification, two specimens of two-meters length were tested. The specimens details are shown in **Fig. 23**. Each specimen was reinforced with two 10 mm deformed bars. A 20 mm-thick steel plate was punched as shown in **Fig. 23** and **Fig. 24**, and the main reinforcement was attached to the plate by means of nuts. A PC tendon was attached to the center of the plate by a nut as also shown in **Fig. 23** and **Fig. 24**. The test machine load was applied directly to this tendon. Specimen elongation was measured by a box-type displacement transducer fixed to the steel plate, as illustrated in **Fig. 23**.

The specimens cross sections, reinforcement, and concrete cover were identical. However, one of them had no hoops, while the other was transversely reinforced with 6 mm hoops (Fig. 23 and Fig. 25) The ratio of cover to bar diameter in both specimens was 1.0, which would give no tension stiffening and no transverse cracks according to Abrishami and Mitchell¹⁰. The authors deemed that Abrishami's model might be valid primarily for the cases of shallow depth and insufficient cover on both sides. The specimens tested in this study represent the more common case of large-sized reinforced concrete members. The behavior was expected to be deviant from Abrishami's model, since different confining and bond properties can be expected.

Figures 26 through 29 illustrate the analytical and experimental results. Figures 26 and 28 show the load-elongation relationship, while Figs. 27 and 29 show the tension stiffening of concrete in comparison with Abrishami's model. From these figures, it can be concluded that the author predictions are in a fairly good agreement with the experiment and that Abrishami's model underestimates the tension stiffening.

The analysis indicates a splitting load of 49 kN in specimen (1) and no splitting in specimen (2). The observed splitting load of specimen (1) was 45 kN with a deviation of 8% from the analytical value, while no splitting crack was observed in specimen (2) reinforced with transverse reinforcement as shown in Fig. 30. Also, the predicted crack spacing was close to the experiment with deviation of 12% and 19%, respectively.

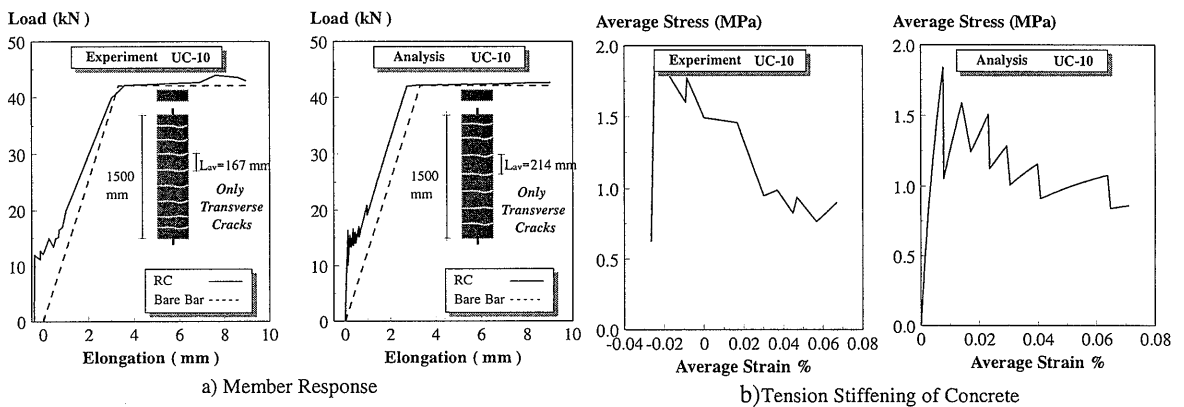


Fig.18 Comparison between authors' analysis and experimental work of Abrishami and Mitchell¹⁰: (Specimen UC-10)

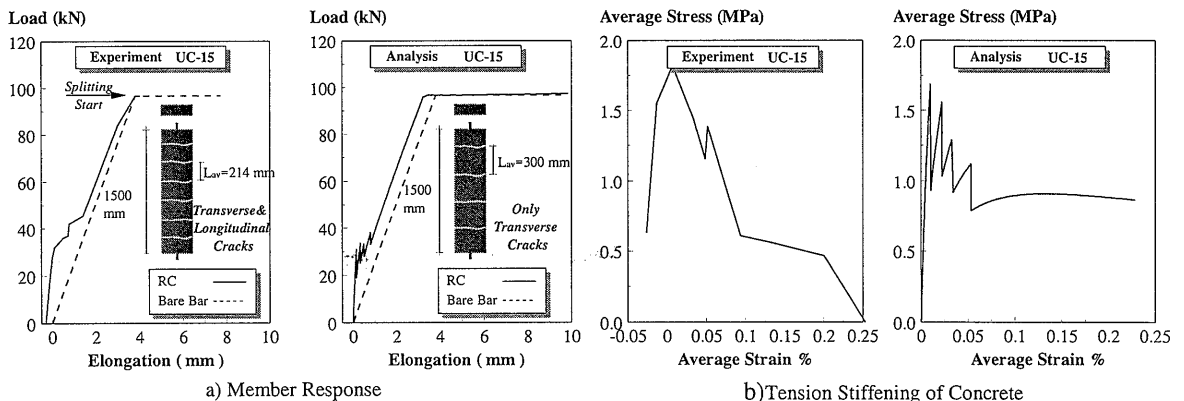


Fig.19 Comparison between authors' analysis and experimental work of Abrishami and Mitchell¹⁰: (Specimen UC-15)

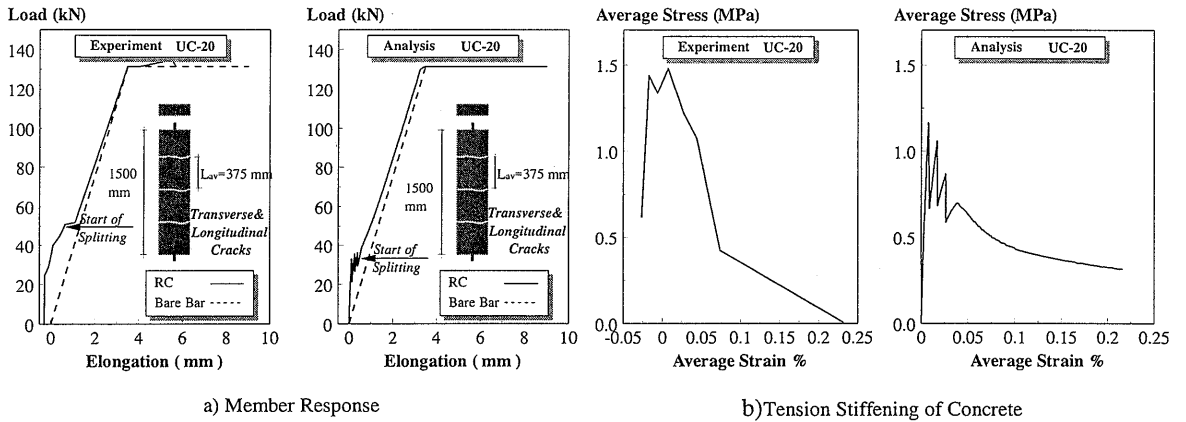


Fig.20 Comparison between authors' analysis and experimental work of Abrishami and Mitchell¹⁰: (Specimen UC-20)

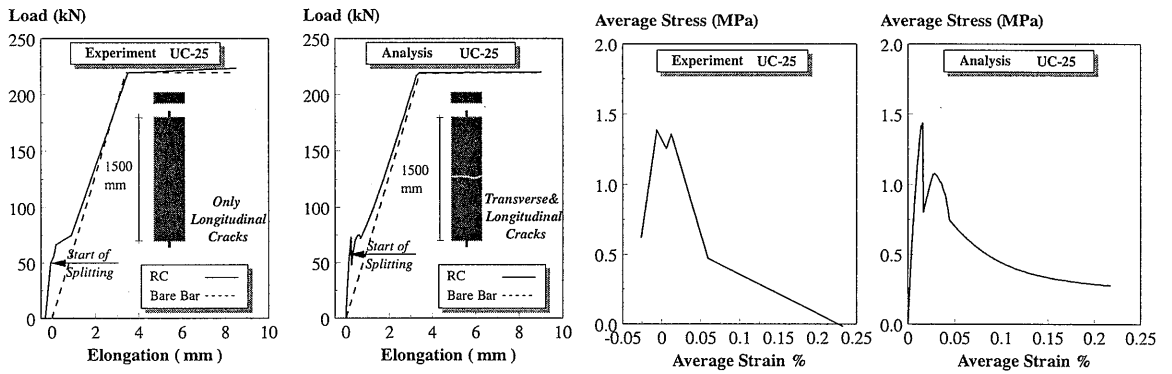


Fig.21 Comparison between authors' analysis and experimental work of Abrishami and Mitchell¹⁰: (Specimen UC-25)

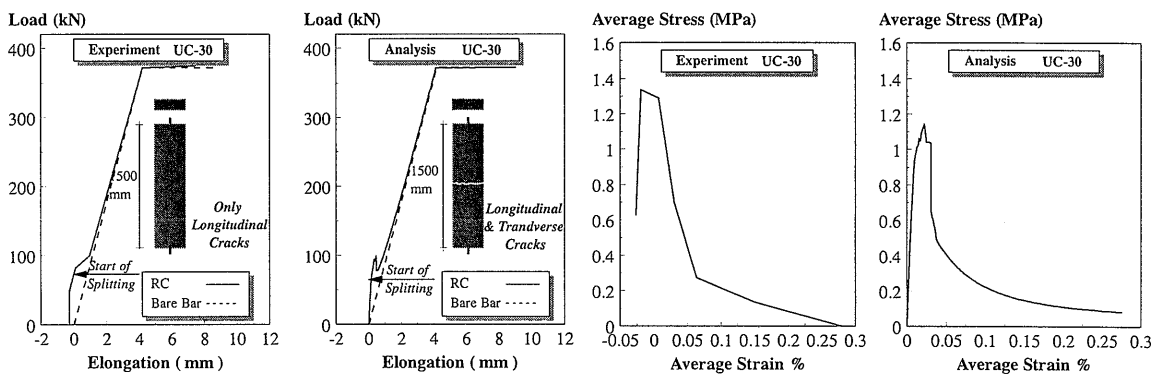


Fig.22 Comparison between authors' analysis and experimental work of Abrishami and Mitchell¹⁰: (Specimen UC-30)

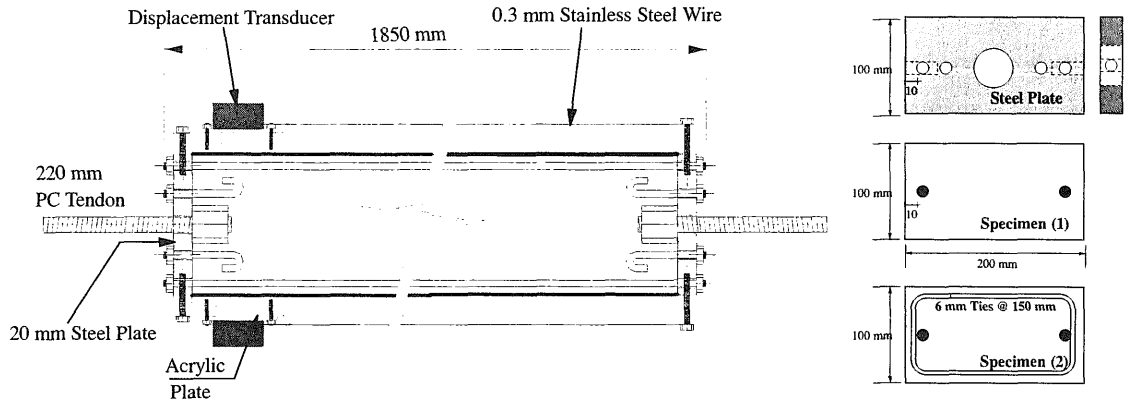


Fig. 23 Details of test specimens

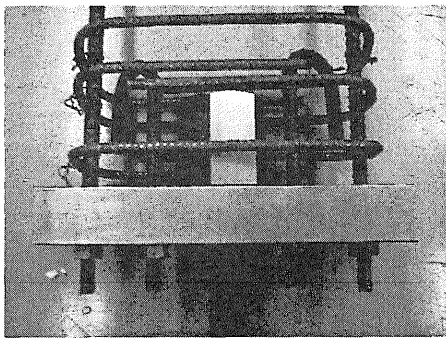


Fig. 24 PC tendon connection to the specimen

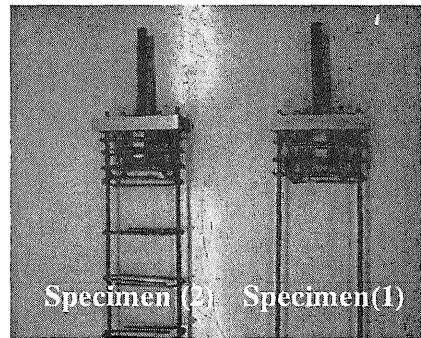


Fig. 25 Reinforcement details of test specimens

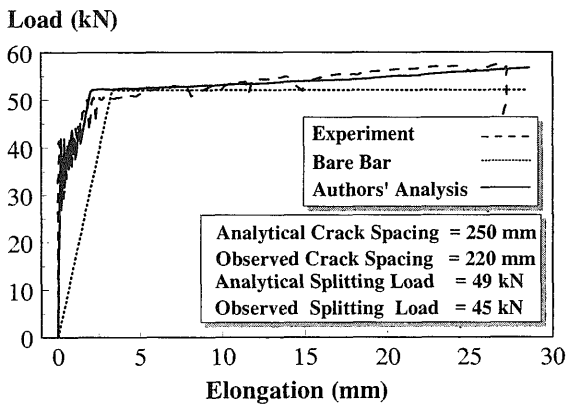


Fig. 26 Results of specimen (1): load-elongation relationship

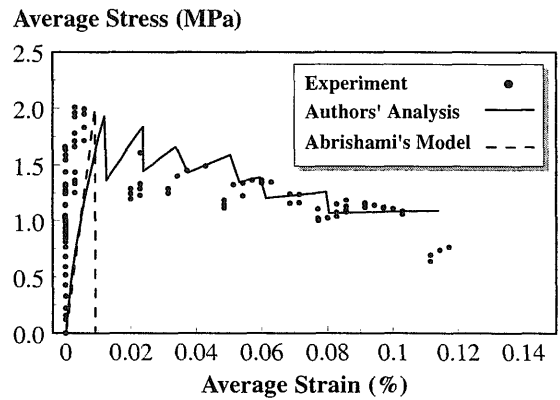


Fig. 27 Results of specimen (1): tension stiffness of concrete (before yielding)

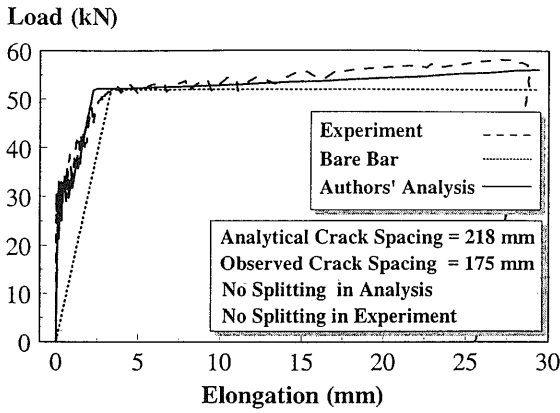


Fig. 28 Results of specimen (2): load-elongation relationship

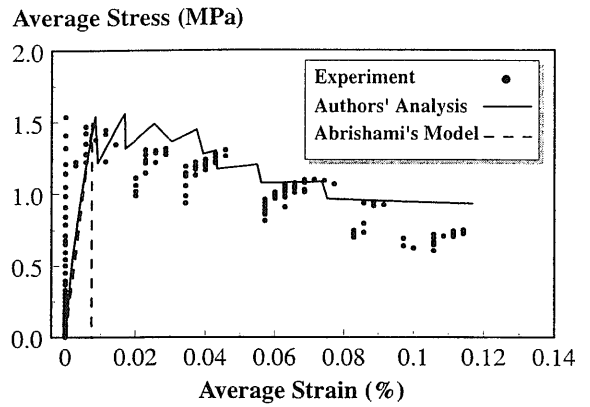


Fig. 29 Results of specimen (2): tension stiffness of concrete (before yielding)

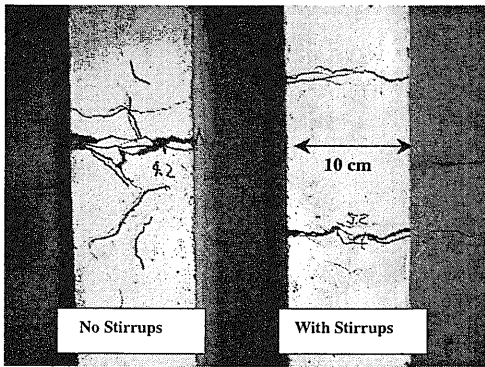


Fig. 30 Observed crack pattern of test specimens

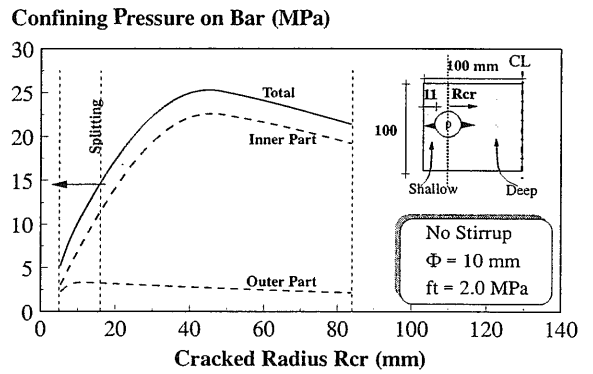


Fig. 31 Confining of bars in specimen (1)

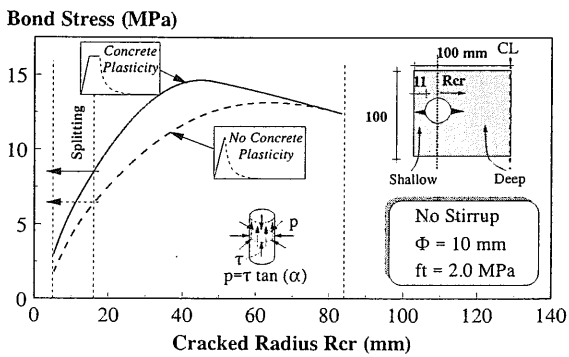


Fig. 32 Concrete plasticity effect on confinement and bond of bars in specimen (1)

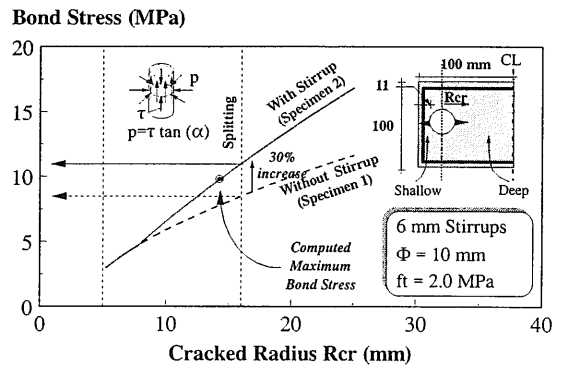


Fig. 33 Bond Stresses of bars in specimen (2)

In the analysis of the two specimens, the bond stresses were not affected by splitting cracks. In fact, the original Shima bond model was used, since Gambarova's model gave bond stresses higher than Shima's model due to the huge confinement of bars even after the occurrence of the splitting cracks. **Figure 31** illustrates the confining pressure on the bars of specimen (1). If we consider the bar cross section as dividing the concrete into two zones, where one is on the shallow side while the other is on the deep side, it can be seen that the confinement of the deep side of concrete is predominant. In Abrishami's experiment, this confining action developing inside the specimen does not exist, leading to the great reduction in bond stresses.

Figure 32 illustrates the computed bond stress on bars in specimen (1) as a function of the cracked radius, both with and without taking the concrete plasticity in tension into consideration. As can be seen from this figure, the effect of concrete plasticity cannot be neglected. If it is neglected, the computed splitting bond stress would be 6.3 MPa instead of 8.4 MPa and the computed splitting load would be 32 kN instead of 49 kN, which is far from the experimental observations.

Figure 33 illustrates the computed bond stress on bars in specimen (2) in comparison with that in the case of specimen (1). Due to the confining action of the steel ties in specimen (2), a 30% increase in bond stress required to cause splitting of the cover is computed. The computed maximum local bond stress in this specimen did not reach the splitting bond stress, as is clear in **Fig. 33**. Based on this, the splitting load increased and no longitudinal cracks were expected. This agrees well with the experimental observations.

7. CONCLUSIONS

Based on the tension softening of plain concrete, the radial bond stresses, and hence the splitting load of tension members with insufficient cover has been predicted.

The effect of splitting cracks on the bond properties and tension stiffening was discussed, and the possible reduction in tension stiffening due to longitudinal cracks has been predicted.

The effect of splitting cracks on the bond properties and tension stiffening is very large for structural members with shallow thickness, such as thin shells, where the concrete cover is insufficient on all sides. However, this effect is negligible for deep structural members, like beams, even if the concrete cover is not sufficient. This is due to the effect of the confining action of concrete on the deep side.

References

- [1] Timoshenko, S.: *Strength of Materials. Part II: Advanced Theory and Problems*, Princeton, N. J., D. Van Nostrand Company Inc., pp. 205-210, 1956.
- [2] Goto, Y.: Cracks formed in concrete around deformed tension bars, *ACI Journal*, Proceedings Vol. 68, No. 4, pp. 244-251, 1971.
- [3] Morita, S. and Kaku, T.: Splitting bond failure of large deformed reinforcing bars, *ACI Journal*, Proceedings Vol. 76, pp. 93-110, 1979.
- [4] Shima, H., Chou, L., and Okamura, H.: Micro and macro models for bond in reinforced concrete, *Journal of The Faculty of Engineering*, The University of Tokyo (B), Vol. 39, No 2, 1987.
- [5] Gambarova, P., Rosati, G., and Zasso, B.: Steel-to-concrete bond after concrete splitting: constitutive laws and interface deterioration, *Materials and Structures*, Vol. 22, pp. 347-356, 1989.
- [6] Okamura, H. and Maekawa, K.: *Nonlinear Analysis and Constitutive Models of Reinforced Concrete*, Gihodo, Tokyo, 1991.
- [7] Uchida, Y., Rokugo, K. and Koyanagi, W.: Determination of tension softening diagrams of concrete by means of bending tests, *Proc. of JSCE*, Vol. 14, No. 426, pp. 203-212, 1991.
- [8] Maekawa, K. and Qureshi, J.: Stress transfer across interfaces in reinforced concrete due to aggregate interlock and dowel action, *Journal of Materials, Concrete Structures and Pavements, JSCE*, Vol.34, No. 557, pp 159-172, 1997.

- [9] A Valle, M., Iori, I. and Vallini, P.: Analisi numerica del comportamento di elementi in conglomerato armato semplicemente tesi, *Studi E Ricerche*, Vol. 14, pp. 29-54, 1993 (*In Italian*).
- [10] Abrishami, H. and Mitchell, D.: Influence of splitting cracks on tension stiffening, *ACI Structural Journal*, Vol.93, No.6, pp. 703-710, 1996.
- [11] Salem, H. and Maekawa, K.: Tension stiffness for cracked reinforced concrete derived from micro-bond characteristics, *Proc. of JCI*, Vol.19, No.2, pp. 549-554, 1997.
- [12] Salem, H. and Maekawa, K.: Computational model for tension stiffness of cracked reinforced concrete derived from micro-bond characteristics, *Proc. Of the Sixth East Asia-Pacific Conference on Structural Engineering & Construction*, Taipei, Vol.3, pp. 1929-1934, 1998.
- [13] Salem, H., Hauke, B. and Maekawa, K.: Concrete cover effect on tension stiffness of cracked reinforced concrete, *Proc. of JCI*, Vol. 20, No.3, pp. 97-102, 1998.
- [14] Bujadham, B., Harada, S. and Maekawa, K.: Temperature and tensile stress path dependent models for tensile strength of concrete, *Proc. of JCI*, Vol.10, No.3, pp. 721-726, 1988.
- [15] Saitoh, S., Yoshii, Y. and Iizima, M.: Anchorage capacity of ribbed steel pipes embedded in concrete, *Proc. of JSCE Annual Convention*, Vol.50, pp. 800-801, 1995.